Thermally Resilient Planar Waveguides in Novel nc-YSZ Transparent Ceramic by *fs* Laser Pulses

Gabriel R. Castillo[1,2], Cecilia Burshtein[2], Gottlieb Uahengo[3], Elías H. Penilla[3], Yasmín Esqueda-Barrón[2], M. Martinez-Gil[4], Wencel de la Cruz[4], Javier E. Garay[3] and Santiago Camacho-López[2]*

[1]Cátedras CONACYT–Centro de Nanociencias y Nanotecnología, Universidad Nacional Autónoma de México, Ensenada, Mexico, [2]Departamento de Óptica, Centro de Investigación Científica y Educación Superior de Ensenada, Ensenada, Mexico, [3]Jacobs School of Engineering Mechanical and Aerospace Engineering, University of California San Diego, San Diego, CA, United States, [4]Centro de Nanociencias y Nanotecnología, Universidad Nacional Autónoma de México, Ensenada, Mexico

We report on thermally resilient planar waveguides fabricated on nc-YSZ by direct fs-laser inscription in transparent nc-yttria stabilized zirconia (nc-YSZ) polycrystalline ceramic. The waveguides consisted of rectangular sections ($4.5 \times 2 \, mm^2$) on the surface of the sample. Optical characterization at 633 and 810 nm was performed. We estimate a laser-induced refractive index contrast of 10^{-4}. Post-waveguide-fabrication thermal annealing treatments at 750°C for 24 h were carried out to test the resilience of the waveguides and to further reduce the waveguide losses. Both micro-Raman spectroscopy and XPS characterization revealed unmodified lattice and steady chemical features, which are consistent with the waveguide thermal resilience. Our results suggest a promising potential use of nc-YSZ in harsh and high temperature demanding photonic environments.

Keywords: laser materials processing, femtosecond lasers, optical waveguides, yttria stabilized zirconia ceramic, biocompatible materials

INTRODUCTION

Optical waveguides have been fabricated for multiple photonic applications and are fundamental in integrated photonics due to their micrometric scale. Different techniques such as ion implantation [1], thin film deposition [2], and direct fs-laser inscription [3–7] for several materials have been developed to achieve optical guiding.

The proven ability of fs-laser processing to create numerous 3D structures for photonic applications, such as enhanced nonlinear responses, waveguide lasers, and photonic lanterns, among others [8–16], place it as one of the most versatile and feasible methods for waveguide fabrication.

Most laser-induced structures have been demonstrated in glasses and single crystals, although more recently some laser structures have been written in polycrystalline YAG [17, 18]. Ceramic materials offer high temperature/chemical stability, superior mechanical toughness as well as greater fabrication flexibility when compared to single crystals but are largely untested.

Polycrystalline yttria stabilized zirconia (YSZ) is broadly recognized as one of the most useful high temperature structural materials due to its ionic conducting properties [19], high-temperature stability [20], record toughness [21], and proven biocompatibility [22]. While these properties make

YSZ a promising material for extreme integrated photonic applications, it is still not in general recognized as an optical material, since most fabrication processes lead to optically opaque YSZ. Recently we developed a process that produces fine nanocrystalline (nc) grain sizes and low porosity leading to optical transparency in YSZ: Current-Activated Pressure-Assisted Densification (CAPAD [17]).

Annealing-related tunable optical properties is another feature obtained through a rapid and relatively efficient fabrication method of nc-ceramics [21] as compared to glasses and single crystals. Their use in waveguide fabrication has not been widespread. However, a method for writing waveguides, in transparent biocompatible nc-YSZ ceramics, using fs laser pulses with very low laser fluence has been already proposed [23]. Using amplified pulses, the necessary power to induce permanent optical changes is similar for both single crystals and ceramics.

Thermal treatment of fs-laser written waveguides at relatively low temperatures has been proven to improve the guiding properties of a waveguide, quantified with an increase of the induced refractive index change (Δn) or waveguide losses reduction [24–27]. Nonetheless, these studies report on both reduction the of Δn and higher measured losses after the annealing times exceed only 2–4 h at a higher maximum temperature of 700°C.

Waveguides fabricated below ablation threshold in conventional materials such as glasses, single crystals and polymers generally do not stand high annealing temperatures. On the contrary, ceramic materials are high temperature resilient; therefore, written waveguides in this kind of materials can be expected to be robust to high annealing temperatures. Thermally resilient waveguides become very relevant for photonic devices mean to operate in extreme temperature environments in industrial applications.

In this work, we show the first successful demonstration of laser direct writing (LDW) of thermally resilient to high temperature (750°C) planar waveguides. We have characterized the polarization, insertion, and propagation losses of these waveguides at 633 and 810 nm, having tested for the optimal energy required to induce localized structural modifications on the surface of the material. Based on optical microscopy and micro-Raman characterization of the nc-YSZ samples within the native and laser modified regions, we find no evidence of chemical phase changes occurring during LDW.

The ability to fabricate thermally resilient waveguides in an optical grade nc-YSZ ceramic that possesses superior chemical, mechanical, thermal, and biocompability properties to conventional optical polymers, glasses, and single-crystals is very useful for the development of optical devices for harsh/demanding environments.

EXPERIMENTAL SETUP

Waveguide Fabrication

The planar waveguides were inscribed on the surface of custom made 0.8 mm thickness polycrystalline 8% yttria stabilized zirconia (8YSZ) slabs [28], which were polished to optical quality with diamond abrasive of grain size down to 1 μm. The laser source was an Yb fiber laser (Satsuma HP2, Amplitude Systemes) producing 270 fs pulses at a central wavelength of 1,030 nm at 1 MHz repetition rate. The per pulse energy was set to 2 μJ with the help of a half-wave plate and a cube linear polarizer; the scanning speed was kept constant at 500 μm/s.

Using a computer controlled XYZ translation stage system with submicron spatial resolution and an aspherical lens with numerical aperture (NA) of 0.75, laser inscription was executed by translating the YSZ samples with respect to the focused laser beam (FWHM ≈3.8 μm) on the surface of the samples. This creates waveguides ≈30 μm below surface. For the waveguides a set of 200 lines separated by 10 μm was inscribed along the 4,500 μm side of the sample; every line consists of 10 laser scans. This technique forms a 2000 × 4,500 μm² square with a positive Δn in the fs-laser focal volume.

Transmittance measurements of the processed and unprocessed region of the nc-YSZ sample with a waveguide were carried out before and after an annealing in air procedure 750°C in a furnace for 24 h. This annealing process induces transparency into the nc-YSZ sample by removing oxygen vacancies within the bulk material [21].

Optical Waveguide Characterization

Supported spatial propagation modes of the waveguide, their insertion losses, together with their polarization dependence were obtained by coupling a He-Ne laser at 633 nm into the waveguide. To couple the beam, a ×10 microscope objective was focused on the input face of the sample and positioned into the waveguide with the help of a XYZ submicron positioning system. At the end-face, a ×20 microscope objective and a CCD camera were used to retrieve the propagating modes. Likewise, a 810 nm Ti:sapphire laser was used to acquire modal profiles and propagation losses of the waveguides. Only the modal profiles and insertion losses at $\lambda \approx 633$ nm were measured before and after annealing for comparison purposes; the remaining characterization was performed after annealing.

A polarization analysis of the waveguide was carried out employing a halfwave plate to control the polarization of the incident He-Ne laser beam and recording the output power at every position of the plate. This measurement helps to assess whether the guiding features are input polarization independent. A second analysis was performed, although this time adding a polarizer as an analyzer at the output of the waveguide. Again, the output power at every position of the plate was recorded. This approach verifies if propagation through the waveguide modifies the polarization state of the incident beam. These measurements were taken after annealing.

Micro-Raman Measurements

In order to obtain information about the effects that ultrahigh irradiance fs-laser pulses have on the crystal phase of the YSZ ceramic, micro-Raman measurements across the laser processed region were carried out. For this purpose, a Horiba Scientific X´plora microRaman system with a laser at 532 nm was employed;
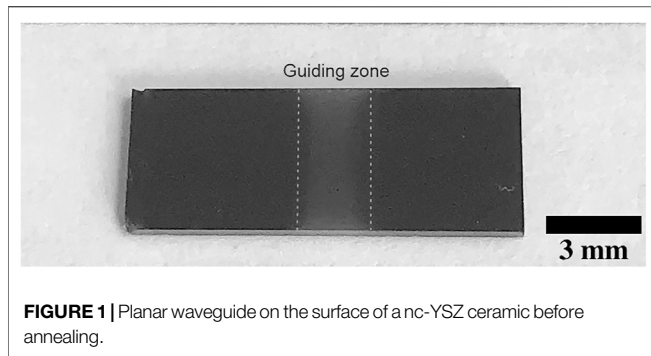
FIGURE 1 | Planar waveguide on the surface of a nc-YSZ ceramic before annealing.

the laser beam was focused on the sample with a 10X microscope objective, the spatial resolution of the system is 3 μm (FWHM). Spectra from two distinct zones were recorded to identify any laser-induced modification to the crystalline structure of the YSZ ceramic: measurements were taken on the unprocessed region, and in the guiding zone. Again, these measurements were taken after annealing.

X-Ray Photoelectron Spectroscopy

The surface elemental composition of the samples (both the irradiated and non-irradiated zones and to analyze the effect of femtosecond laser over the YSZ sample) was analyzed on a Specs X-ray photoelectron spectrometer with monocromatized Al Ka radiation (1,486.6 eV). The base pressure of the instrument was 10–10 Torr. Survey scans were obtained in the 1,400 to 0 eV energy interval at 1.0 eV per step, pass energy of 100 eV. Additionally, the high-resolution XPS scans were completed at 0.2 eV energy steps and pass energy of 20 eV (constant pass energy mode). These detailed scans were recorded for the Zr2d, C1s, Y2p, and O1s for the samples. All binding energy (BE) measurements were corrected for charging effects with reference to the C1s peak at 2,845.5 eV using an electron flood gun. This reference gave BE values with an accuracy of 0.2 eV. Collected data were analyzed with Tougaard background subtraction, which was performed with a Gaussian profile. For quantitative analysis, the signal intensities were measured by using the integrated area under the detected peak. To evaluate the surface atomic ratios, we used as sensitivity factors the cross-section for X-ray excitation calculated by Scofield [29]. They are 5.14, 2.44, and 2.93 for Zr 3p3/2, Y 3p3/2, and O1s, respectively.

Thermal Annealing

Post-waveguide fabrication thermal annealing treatments at 750°C for 24 h were carried out to test the resilience of the waveguide, to increase the transmittance of the nc-YSZ samples, and to improve the optical performance of the waveguide by removing color centers. It is well known that the so-called Type I modification waveguides, where direct laser written tracks are formed, are weak modifications which usually vanish at high temperatures [16]; the induced refractive index change can be either positive or negative according to the material properties. However, our waveguides are thermally resilient at the mentioned record temperature.
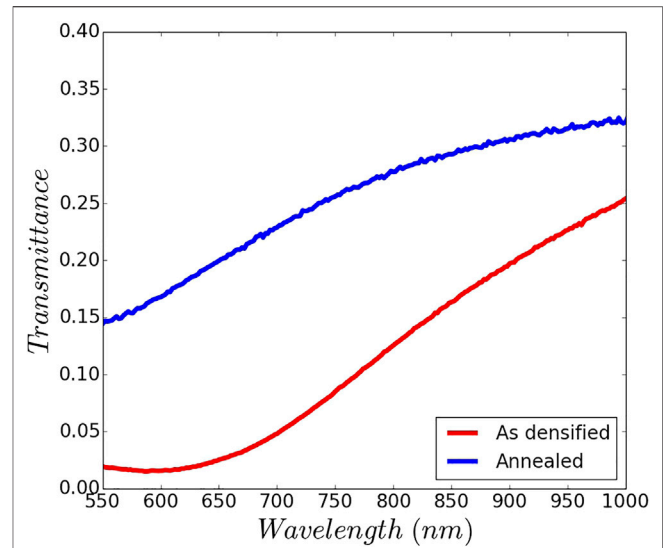

FIGURE 2 | As densified and 24 h annealed transmittance measured at a region in the nc-YSZ ceramic far away from the laser written planar waveguide.
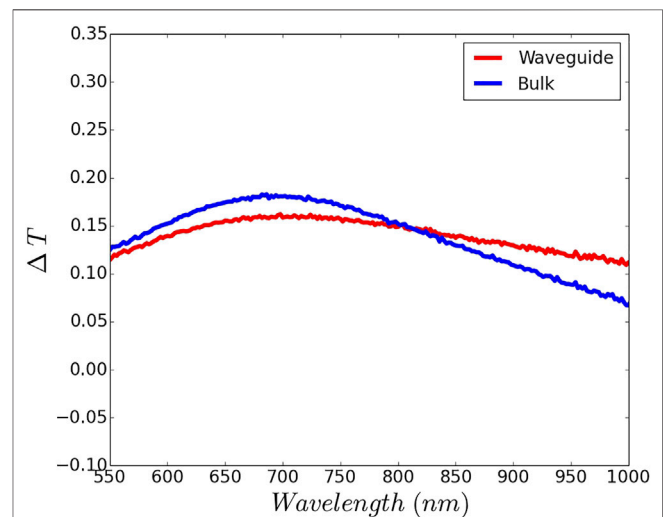
FIGURE 3 | nc-YSZ transmittance changes after 24 h annealing at the waveguide zone and at a region far away from waveguide zone within the same sample.
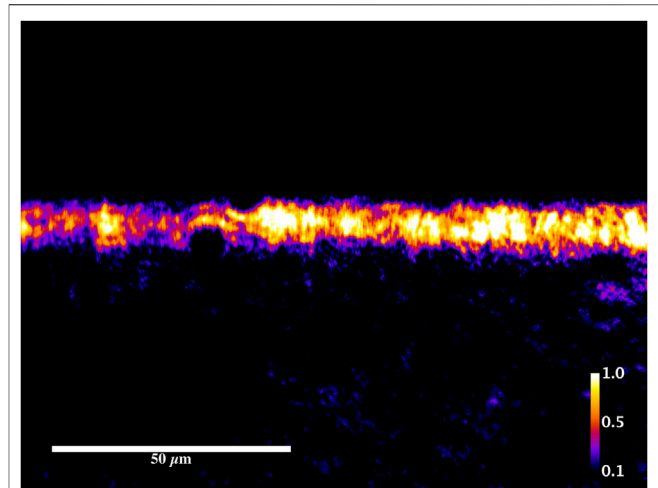
RESULTS AND DISCUSSION

About the guiding regions, they appear as light colored well defined square zones with no ruptures or fractures neighboring them, and they are generated as a result of a positive refractive index change in the irradiated focal volume (**Figure 1**). There is a significant difference in the appearance of the samples after annealing in air. The samples were dark gray color when fabricated, but after annealing they became lighter due to oxygen diffusion into the material, which suppresses color
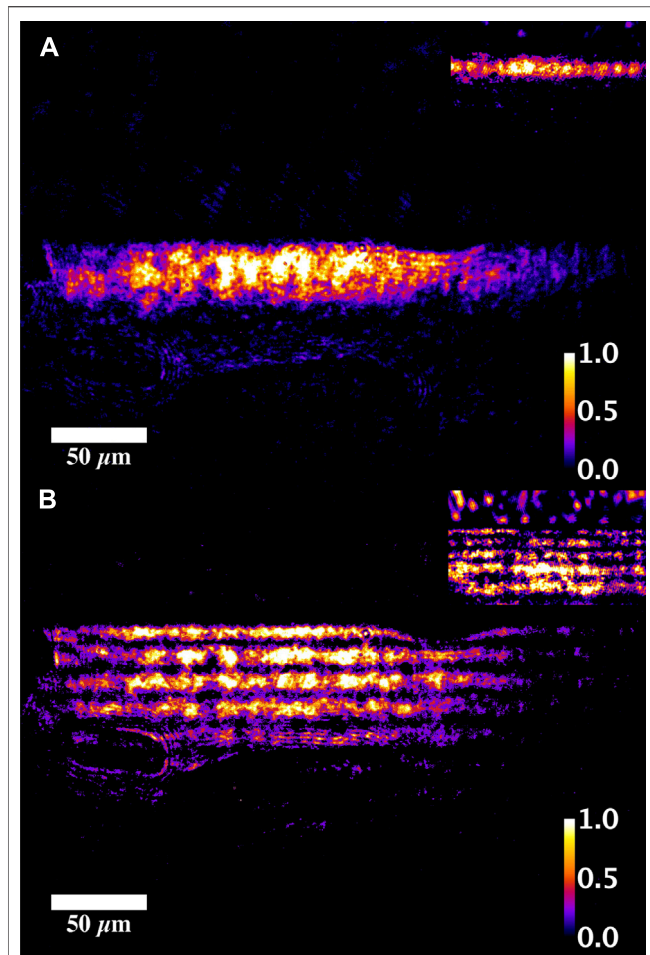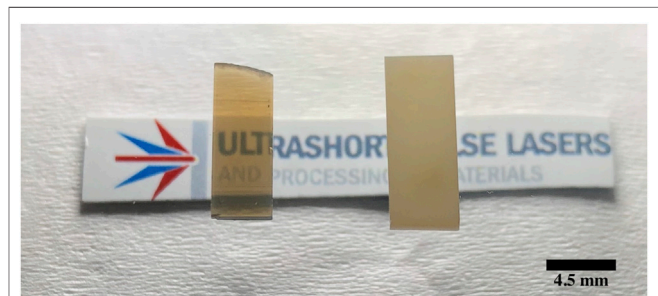
FIGURE 4 | Spatial propagating modes at 633 nm of the planar waveguide in the nc-YSZ ceramic after 24 h of annealing in air. **(A)** TE polarization single-mode propagation, **(B)** TE polarization multi-mode propagation. The inset pictures in this figure show the propagating modes prior to annealing.

FIGURE 5 | Spatial propagating TE mode at 810 nm of the planar waveguide in the nc-YSZ ceramic after 24 h of annealing in air.

FIGURE 6 | nc-YSZ samples with planar waveguides after 24 h of annealing in air.

centers. It has been shown for the case of YSZ that as the annealing time is increased, its optical transmission T enhances while the absorption coefficient decreases [28]. Transmittance measurements confirm that after 24 h of annealing, the transmission of both the laser processed and the non-laser processed regions increases at all measured wavelengths (**Figure 2**).

Changes in transmittance ΔT for both regions are wavelength dependent, and as seen in **Figure 3**, the increase in transmittance for the waveguide is significantly higher than in the non-laser irradiated bulk material for the near IR region. It is important to point out that transmittance was measured using a spectrophotometer with an incident light beam propagating normal to the surface of the sample. One of the measurements was carried out within the fs laser irradiated zone (i.e., the waveguide zone), and a second one measurement was performed in the YSZ sample at a faraway position from the fs laser irradiated zone. So that we are comparing the transmittance of the sample between the laser processed YSZ and the non-laser processed YSZ.

Furthermore, the end-face viewing setup reveals that the near field intensity distribution is consistent with a planar waveguide, on the other hand, the waveguide can be excited to propagate either in single-mode or multi-mode. Waveguiding is supported for both TE and TM incident polarized light. **Figure 4** depicts the propagating modes at 633 nm prior and after 24 h annealing. Guidance in single-mode and multi-mode was also observed at 810 nm; **Figure 5** corresponds to TE single-mode propagation in the nc-YSZ ceramic waveguide after 24 h of annealing in air.

Annealing experiments of the planar waveguides were performed so that transmittance of nc-YSZ is raised. The planar waveguide visually vanished since the entire sample became clearer and transparent as seen in **Figure 6**. Despite this, the direct fs-laser written waveguides remained and in their optical properties improved. Such temperature stability suggests that Δn is caused not only by cumulative laser induced thermal effects but other physical processes are involved [23].

Thermal annealing has been previously found to diminish the waveguides propagation losses and to increase the laser induced

TABLE 1 | Temperature values (°C) and their respective annealing time (in hours) at which fs-laser written waveguides start to vanish according to a Δn decrease or increasing propagation losses criteria.

| Material	Type	Temperature (°C)	Annealing Time (hours)	Waveguide type	Waveguide vanishing criteria
crystal	$Bi_4Ge_3O_{12}$	260	2	cladding	Δn decrease and higher propagation losses [24]
glass	$CaSio_3$ - $Ca_3(PO_4)_2$	650	0.5	cladding	higher propagation losses [25]
crystal	$LiNbO_3$	300–500	6	cladding	higher propagation losses [26]
crystal	$LiNbO_3$	700	3	cladding	Δn decrease [27]
ceramic	nc-YSZ	750	24	directly written	no Δn decrease or higher propagation losses observed [this work]

TABLE 2 | Measured insertion losses at 633 nm prior and after 24 h annealing in air for TE and TM polarized incident light.

Polarization	Before	After
TM	27.21 ± 1 dB	15.68 ± 1 dB
TE	29.58 ± 1 dB	16.02 ± 1 dB

Δn by several studies, some of which are summarized in **Table 1**. It is worth noting that although the waveguides optical properties have been demonstrated to improve with thermal treatments, none of these studies have reached temperatures as high as our waveguides underwent, nor for as long.
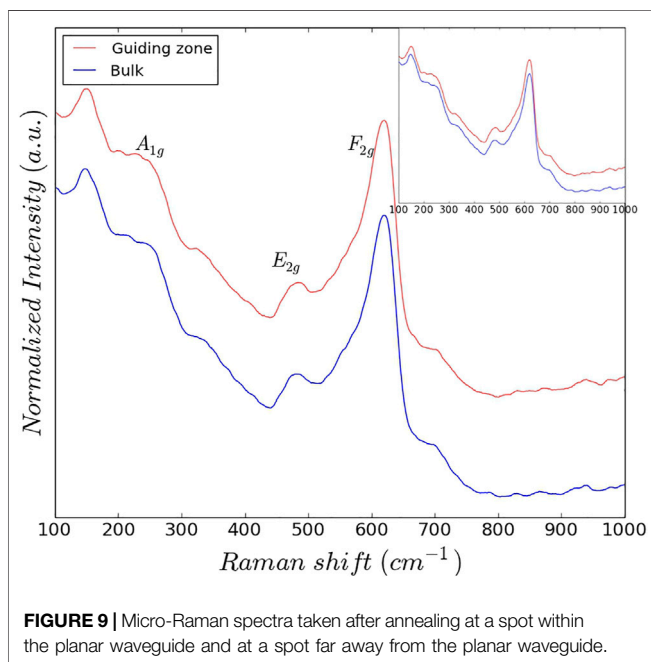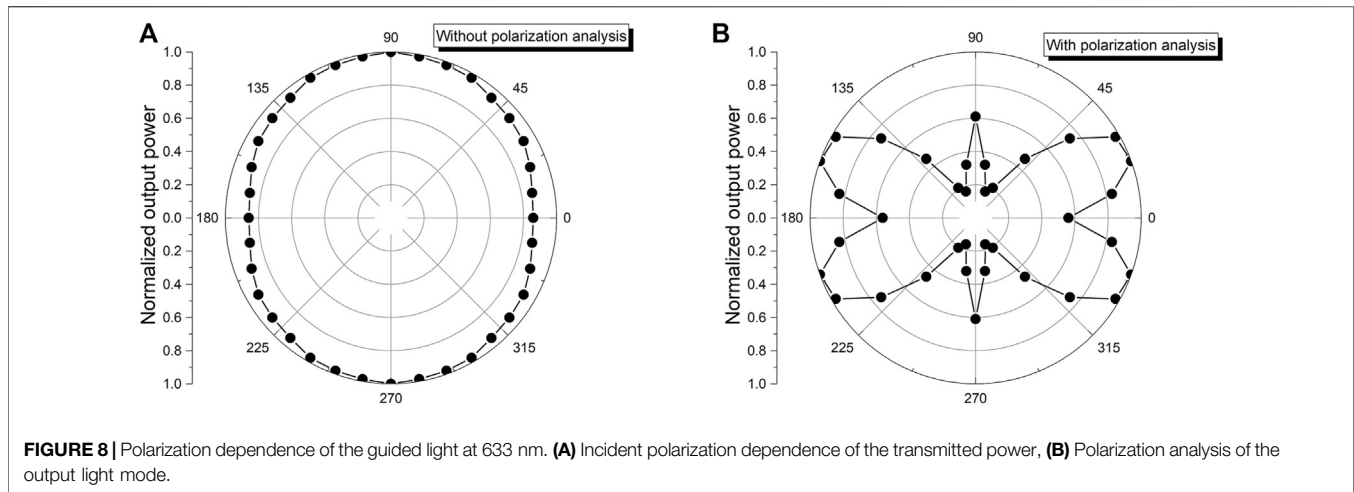
Respecting the insertion losses, presented in **Table 2**, they were estimated by collecting the output of the waveguides with the coupling experimental setup. Current high losses are attributed to linear optical absorption caused by oxygen vacancies inherent to the sample fabrication, as discussed earlier. Nevertheless, it is possible that these losses can be mitigated by putting the sample through an extended annealing procedure in air or by tuning the fabrication parameters to cause fewer defects (oxygen vacancies). Propagation losses at 633 and 810 nm were also measured applying the scattered light imaging method [30, 31], giving 11.5 dB/cm and 9.5 dB/cm for 633 and 810 nm, respectively; indicating our waveguides are more efficient for longer wavelengths. We probe different laser irradiation parameters for the fabrication of the waveguides, and we did not observe considerable changes in the transmission of the resulting waveguides. We found two uJ was the optimum energy to ensure the successful inscription of the waveguides while keeping the damage of the material within a reasonable level such that cracks or other physical defects are not produced. This nc-YSZ ceramic material is still under active research aiming the optimization of its optical quality by tailoring both the linear absorption and scattering during the synthesis and post treatment. We must notice though that even at the current relatively large propagation losses, this material offers in return very attractive unmatched features (mechanical toughness, chemical and thermal stability, biocompatibility) when compared against commonly used optical materials for photonics.

Concerning the refractive index contrast Δn between the unprocessed region and the irradiated zone, we applied a finite element analysis [32] to quantify the refractive index contrast of the planar waveguides using a $n = 2.2$ for the bulk material. We
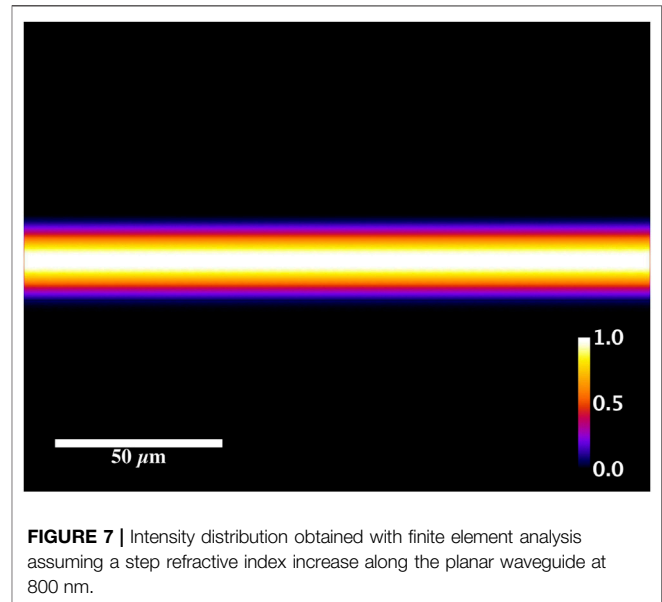
FIGURE 7 | Intensity distribution obtained with finite element analysis assuming a step refractive index increase along the planar waveguide at 800 nm.

accomplished this by comparing the theoretically allowed propagating spatial modes, assuming different Δn values, with those observed experimentally. Chosen Δn values correspond to previously measured Δn induced by fs-laser irradiation in ceramic materials [9, 13, 17, 33]. The results, depicted in **Figure 7**, indicate a contrast of $\Delta n \approx 10^{-4}$ between the written waveguides and the unprocessed material, which is in good agreement with other previously reported fs-laser induced refractive index changes in ceramic materials [9, 13, 17, 33]. By direct comparison between **Figure 7** and **Figure 5**, it is possible to confirm a very good agreement between the simulated and the experimentally measured waveguide output modes.

Regarding the polarization analysis of the waveguides, it was found that although the output intensity of guided light is incident polarization dependent, the planar waveguide is able to guide light in either TE or TM polarization as it is shown in **Figure 8A**. When an analyzer was placed at the output of the waveguides it was also found they exhibit a rather complex anisotropic behavior, showing the polarization of incident light is not preserved along propagation, as it can be clearly seen in **Figure 8B**. In both figures, 0° and 90° correspond to TE and TM polarized incident light, respectively.

FIGURE 8 | Polarization dependence of the guided light at 633 nm. (A) Incident polarization dependence of the transmitted power, (B) Polarization analysis of the output light mode.

FIGURE 9 | Micro-Raman spectra taken after annealing at a spot within the planar waveguide and at a spot far away from the planar waveguide.

In order to determine whether the laser processing induces chemical phase changes and/or decreased crystallinity we implemented micro-Raman spectroscopy. **Figure 9** show the Raman spectra for the native nc-YSZ in regions far from any laser processing compared to the collected spectra within the waveguide. The spectra are normalized and stacked by an offset for better appreciation, while in the inset figures they are seen without normalization to show the spectra of the waveguides have an increased intensity. Comparison of these spectra show no significant softening in the Raman breathing modes (F_{2g}, E_{2g}, A_{1g}) for YSZ [34], which suggest that the laser processing does not induce chemical phase changes. This is expected as YSZ is well known for its chemical stability.
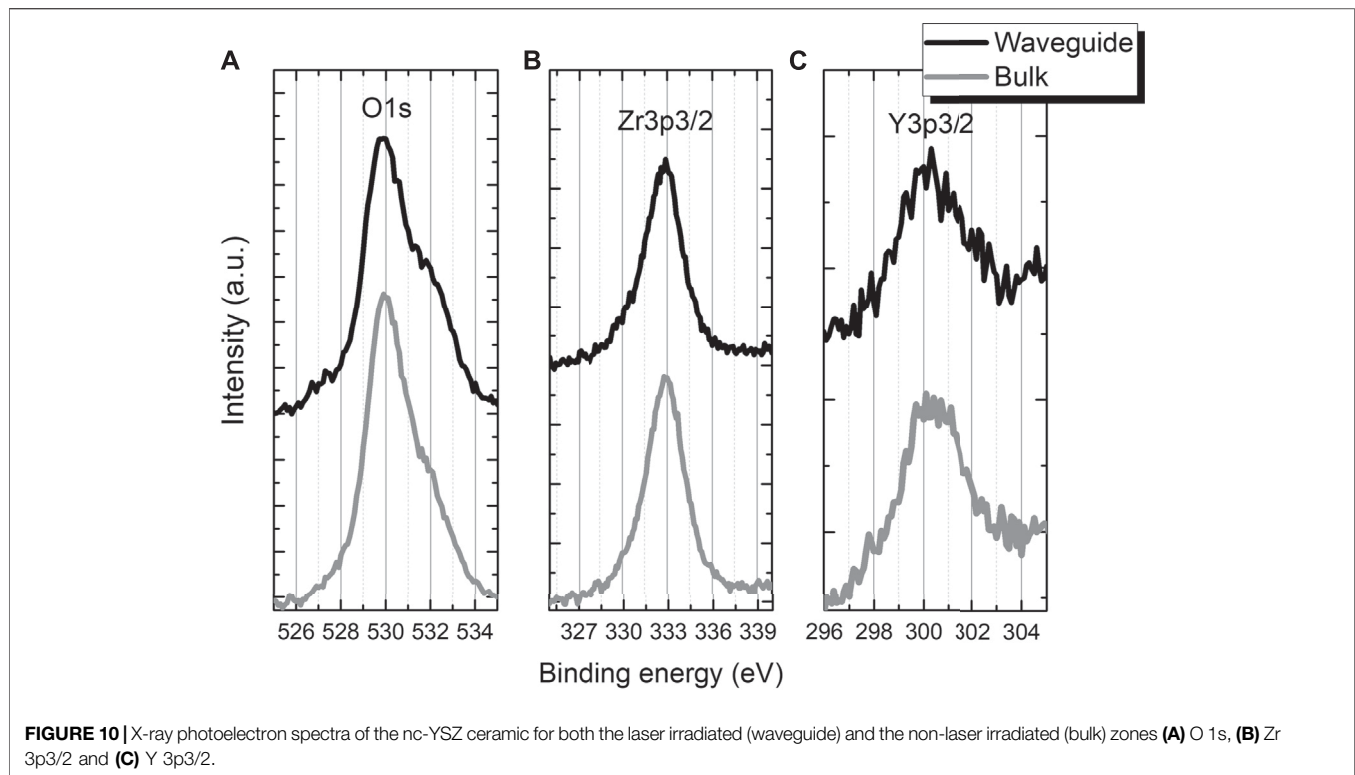
Recently, it was demonstrated that heat treatments up to 700 °C of depressed cladding waveguides in Lithium Niobate

increases the Δn of tracks generated with fs-laser pulses [27]. Since Δn varies with the annealing temperature, it is suggested the bulk and the modified material act as two different materials whose dilation coefficients differ from each other. However, for the nc-YSZ case, micro-Raman spectroscopy indicates that fs-laser processing does not modify the crystalline structure and hence the bulk material and the guiding region cannot be seen as materials with different crystal structures. Instead, we believe that the Δn in YSZ waveguides are caused by oxygen related point defect groups as we discussed earlier [23].

Concerning the XPS analysis **Figure 10** shows the general spectra of the YSZ taken over the irradiated and non-irradiated zones. At first, we did not find a relevant shifting in the position of the peaks for the different zones. Therefore, there are no significant changes in the chemical composition of the ceramic after laser irradiation. Additionally, the atomic concentrations were determined by carrying out a component fitting to each signal. Once again, we did not find relevant difference between concentration percentages for both zones. In conclusion, the XPS spectra are similar in the YSZ bulk and the waveguide region, i.e., the same peaks characteristic of Zr, Y, and O and are found in both. There is not a detectable peak shift between the two spectra indicating there is no detectable change in chemical bonding between elements. It is important to point out that XPS signals are sensitive to distances from the surface so that peak intensity differences might be affected by the differences in waveguide depth.

CONCLUSION

In conclusion, thermally resilient planar waveguides written by direct fs-laser inscription have been demonstrated in the nc-YSZ ceramic with a simulated refractive index contrast of 10^{-4}. The planar waveguide consists in a 2000 by 4,500 μm square region of the sample. It was found that the waveguides can be excited to propagate in either single-mode or multi-mode for TE and TM polarized incident light at 633 or 810 nm. The polarization of the guided light is not preserved,

FIGURE 10 | X-ray photoelectron spectra of the nc-YSZ ceramic for both the laser irradiated (waveguide) and the non-laser irradiated (bulk) zones **(A)** O 1s, **(B)** Zr 3p3/2 and **(C)** Y 3p3/2.

indicating a strong and rather complex induced anisotropy. Micro-Raman and XPS analysis of the laser inscribed waveguide and the non-laser processed nc-YSZ bulk reveals that both the crystalline phase and chemical composition are not compromised by the ultrahigh intensity of the femtosecond laser pulses during waveguide fabrication. Finally, we can confidently state that planar waveguide structures fabricated using fs laser pulses in optically grade nc-YSZ, offer promising potential for tackling challenging photonic applications in harsh (high temperature, extreme pressure, corrosive) demanding environments.

DATA AVAILABILITY STATEMENT

The raw data supporting the conclusions of this article will be made available by the authors, without undue reservation.

AUTHOR CONTRIBUTIONS

GC—waveguide writing methodology, discussion and writing; CB—waveguide writing methodology, data analysis and writing; GU—YSZ synthesis and analysis; EP—YSZ synthesis, discussion; YE-B—Raman characterization, data analysis; MM—XPS measurements and discussion; WdlC—XPS `characterization and discussion; JEG—Transparent nc-YSZ conceptualization, discussion, review; SC-L—Thermally resilient waveguide conceptualization, discussion, writing, review, editing, funding acquisition.

REFERENCES

1. Flores-Romero E, Vazquez GV, Marquez H, Rangel-Rojo R, Rickards J, and Trejo-Luna R. Planar Waveguide Lasers by Proton Implantation in Nd:YAG Crystals. *Opt Express* (2004) 12:2264. doi:10.1364/OPEX.12.002264

2. Righini GC, and Chiappini A. Glass Optical Waveguides: a Review of Fabrication Techniques. *Opt Eng* (2014) 53:071819. doi:10.1117/1.OE.53.7.071819

3. Davis KM, Miura K, Sugimoto N, and Hirao K. Writing Waveguides in Glass with a Femtosecond Laser. *Opt Lett* (1996) 21:1729. doi:10.1364/OL.21.001729

4. Wu P, Yang S, Ren Y, and Liu H. Beam Splitters Fabricated by Nonlinear Focusing of Femtosecond Laser Writing in Pure YAG Crystal. *Front Phys* (2021) 9:9. doi:10.3389/fphy.2021.719757

5. Yang Q, Liu H, Liu H, HeBin Xu S, Tian, Bin Xu Q, and Wu P. Circular Cladding Waveguides in Pr:YAG Fabricated by Femtosecond Laser Inscription: Raman, Luminescence Properties and Guiding Performance. *Opto-electronic Adv* (2021) 4:20000501–15. doi:10.29026/oea.2021.200005

6. Zhuang Y, Yang Q, Wu P, Zhang W, Ren Y, and Liu H. Vortex Beam Array Generated by a Volume Compound fork Grating in Lithium Niobite. *Results Phys* (2021) 24:104083. doi:10.1016/j.rinp.2021.104083

7. He S, Yang Q, Zhang B, Ren Y, Liu H, Wu P, et al. A Waveguide Mode Modulator Based on Femtosecond Laser Direct Writing in KTN Crystals. *Results Phys* (2020) 18:103307. doi:10.1016/j.rinp.2020.103307

8. Jia Y, Chen F, Vázquez de Aldana JR, Akhmadaliev S, and Zhou S. Femtosecond Laser Micromachining of Nd:GdCOB ridge Waveguides for Second Harmonic Generation. *Opt Mater* (2012) 34:1913–6. doi:10.1016/J.OPTMAT.2012.05.032

9. Siebenmorgen J, Petermann K, Huber G, Rademaker K, Nolte S, and Tünnermann A. Femtosecond Laser Written Stress-Induced Nd:Y3Al5O12 (Nd:YAG) Channel Waveguide Laser. *Appl Phys B* (2009) 97:251–5. doi:10.1007/s00340-009-3697-3

10. Calmano T, Paschke A-G, Siebenmorgen J, Fredrich-Thornton ST, Yagi H, Petermann K, et al. Characterization of an Yb:YAG Ceramic Waveguide Laser, Fabricated by the Direct Femtosecond-Laser Writing Technique. *Appl Phys B* (2011) 103:1–4. doi:10.1007/s00340-011-4485-4

11. Salamu G, Jipa F, Zamfirescu M, and Pavel N. Cladding Waveguides Realized in Nd:YAG Ceramic by Direct Femtosecond-Laser Writing with a Helical Movement Technique. *Opt Mater Express* (2014) 4:790. doi:10.1364/OME.4.000790

12. Zhang C, Dong N, Yang J, Chen F, Vázquez de Aldana JR, and Lu Q. Channel Waveguide Lasers in Nd:GGG Crystals Fabricated by Femtosecond Laser Inscription. *Opt Express* (2011) 19:12503–8. doi:10.1364/OE.19.012503

13. Okhrimchuk AG, Shestakov AV, Khrushchev I, and Mitchell J. Depressed Cladding, Buried Waveguide Laser Formed in a YAG:Nd3+ crystal by Femtosecond Laser Writing. *Opt Lett* (2005) 30:2248–50. doi:10.1364/OL.30.002248

14. Torchia GA, Ródenas A, Benayas A, Cantelar E, Roso L, and Jaque D. Highly Efficient Laser Action in Femtosecond-Written Nd:yttrium Aluminum Garnet Ceramic Waveguides. *Appl Phys Lett* (2008) 92:111103–142. doi:10.1063/1.2890073

15. Birks TA, Gris-Sánchez I, Yerolatsitis S, Leon-Saval SG, and Thomson RR. The Photonic Lantern. *Adv Opt Photon* (2015) 7:107–67. doi:10.1364/AOP10.1364/aop.7.000107

16. Chen F, and de Aldana JRV. Optical Waveguides in Crystalline Dielectric Materials Produced by Femtosecond-Laser Micromachining. *Laser Photon Rev* (2014) 8:251–75. doi:10.1002/lpor.201300025

17. Liu H, Jia Y, Vázquez de Aldana JR, Jaque D, and Chen F. Femtosecond Laser Inscribed Cladding Waveguides in Nd:YAG Ceramics: Fabrication, Fluorescence Imaging and Laser Performance. *Opt Express* (2012) 20:18620–9. doi:10.1364/oe.20.018620

18. Salamu G, Voicu F, Jipa F, Zamfirescu M, Dascalu T, and Pavel N. Laser Emission from Diode-Pumped Nd:YAG Cladding Waveguides Obtained by Direct Writing with a Femtosecond-Laser Beam. *Laser Sourc Appl* (2014) 9135:91351F. doi:10.1117/12.2052250

19. Tuller H. Ionic Conduction in Nanocrystalline Materials. *Solid State Ionics* (2000) 131:143–57. doi:10.1016/S0167-2738(00)00629-9

20. Zambrano DF, Barrios A, Tobón LE, Serna C, Gómez P, Osorio JD, et al. Thermal Properties and Phase Stability of Yttria-Stabilized Zirconia (YSZ) Coating Deposited by Air Plasma Spray onto a Ni-Base Superalloy. *Ceramics Int* (2018) 44:3625–35. doi:10.1016/j.ceramint.2017.11.109

21. Casolco SR, Xu J, and Garay JE. Transparent/translucent Polycrystalline Nanostructured Yttria Stabilized Zirconia with Varying Colors. *Scripta Materialia* (2008) 58:516–9. doi:10.1016/j.scriptamat.2007.11.014

22. Damestani Y, Reynolds CL, Szu J, Hsu MS, Kodera Y, Binder DK, et al. Transparent Nanocrystalline Yttria-Stabilized-Zirconia Calvarium Prosthesis. *Nanomedicine: Nanotechnology, Biol Med* (2013) 9:1135–8. doi:10.1016/j.nano.2013.08.002

23. Castillo-Vega GR, Penilla EH, Camacho-López S, Aguilar G, and Garay JE. Waveguide-like Structures Written in Transparent Polycrystalline Ceramics with an Ultra-low Fluence Femtosecond Laser. *Opt Mater Express* (2012) 2:1416–24. doi:10.1364/OME.2.001416

24. He R, An Q, Vázquez de Aldana JR, Lu Q, and Chen F. Femtosecond-laser Micromachined Optical Waveguides in Bi4Ge3O12 Crystals. *Appl Opt* (2013) 52:3713. doi:10.1364/AO.52.003713

25. Martínez de Mendívil J, Sola D, Vázquez de Aldana JR, Lifante G, De Aza AH, Pena P, et al. Ultrafast Direct Laser Writing of Cladding Waveguides in the 0.8CaSiO3-0.2Ca3(PO4)2 Eutectic Glass Doped with Nd3+ Ions. *J Appl Phys* (2015) 117:043104. doi:10.1063/1.4906963

26. Nguyen H-D, Ródenas A, Vázquez de Aldana JR, Martín G, Martínez J, Aguiló M, et al. Low-loss 3D-Laser-Written Mid-infrared LiNbO_3 Depressed-index Cladding Waveguides for Both TE and TM Polarizations. *Opt Express* (2017) 25:3722–36. doi:10.1364/oe.25.003722

27. Piromjitpong T, Dubov M, and Boscolo S. High-repetition-rate Femtosecond-Laser Inscription of Low-Loss Thermally Stable Waveguides in Lithium Niobate. *Appl Phys A* (2019) 125:302. doi:10.1007/s00339-019-2609-6

28. Alaniz JE, Perez-Gutierrez FG, Aguilar G, and Garay JE. Optical Properties of Transparent Nanocrystalline Yttria Stabilized Zirconia. *Opt Mater* (2009) 32:62–8. doi:10.1016/j.optmat.2009.06.004

29. Scofield JH. Hartree-Slater Subshell Photoionization Cross-Sections at 1254 and 1487 eV. *J Electron Spectrosc Relat Phenomena* (1976) 8:129–37. doi:10.1016/0368-2048(76)80015-1

30. Wang F. Precision Measurements for Propagation Properties of High-Definition Polymer Waveguides by Imaging of Scattered Light. *Opt Eng* (2008) 47:024602–0246024. doi:10.1117/1.2842390

31. Jenkins MH, Phillips BS, Zhao Y, Holmes MR, Schmidt H, and Hawkins AR. Optical Characterization of Optofluidic Waveguides Using Scattered Light Imaging. *Opt Commun* (2011) 284:3980–2. doi:10.1016/j.optcom.2011.04.020

32. Polycarpou AC. *Introduction to the Finite Element Method in Electromagnetics* (2006). doi:10.2200/S00019ED1V01Y200604CEM004

33. Ródenas A, Torchia GA, Lifante G, Cantelar E, Lamela J, Jaque F, et al. Refractive index Change Mechanisms in Femtosecond Laser Written Ceramic Nd:YAG Waveguides: Micro-spectroscopy Experiments and Beam Propagation Calculations. *Appl Phys B* (2009) 95:85–96. doi:10.1007/s00340-008-3353-3

34. Ghosh S, Teweldebrhan D, Morales JR, Garay JE, and Balandin AA. Thermal Properties of the Optically Transparent Pore-free Nanostructured Yttria-Stabilized Zirconia. *J Appl Phys* (2009) 106:113507. doi:10.1063/1.3264613